

Research Report

Resonant Dielectric Gratings for the Control of Light Propagation and Thermal Radiation

Kota Ito, Takayuki Matsui and Hideo Iizuka

Report received on Dec. 23, 2014

■ABSTRACT■ Resonant dielectric gratings have been proposed as promising building blocks for light control. Here we give an overview of our recent studies on resonant dielectric gratings. Firstly, we present an asymmetric grating that exhibits unique reflection and transmission characteristics. Then, resonant modes in gratings coupled to surface modes of specific substrates are demonstrated to control thermal radiation characteristics. These studies pave the way to novel optical and thermal engineering applications.

■KEYWORDS■ Nanophotonics, Subwavelength Gratings, Resonant Dielectric Gratings, Guided Mode Resonance, Thermal Radiation, Asymmetry, Active Modulation, Modal Analysis

1. Introduction

Gratings are optical devices with periodic ridges and grooves. They have been commonly used in spectrometers, because the diffraction angle is dependent on the wavelength. Owing to advances in nanofabrication technologies, gratings whose period is smaller than or comparable to the wavelength have been investigated, and they are called subwavelength gratings. Our company has studied subwavelength gratings⁽¹⁻⁷⁾ and they are summarized as reviews.^(8,9) Some subwavelength gratings composed of dielectric materials exhibit resonant reflection or transmission characteristics with efficiencies as high as unity.⁽¹⁰⁻¹³⁾ Such dielectric resonant gratings have been applied to reflection filters,⁽¹⁰⁻¹⁴⁾ transmission filters,⁽¹⁵⁾ lasers,^(16,17) and lenses,⁽¹⁸⁾ taking advantage of simple configuration, high efficiency, and resonant characteristics. Furthermore, the resonant characteristics could be explained as the excitation of a guided mode in the grating layer.^(12,13) This explanation opens up new design strategies.

Here we introduce our recent theoretical studies on dielectric resonant gratings. In Section 2, we briefly explain a methodology to characterize the optical response of gratings. An asymmetric double-groove grating⁽⁵⁾ that exhibits unique diffraction phenomena is presented in Section 3. In Section 4, dielectric resonant gratings are utilized to control thermal radiation.⁽⁶⁾ The novel coupling mechanism

between guided modes in resonant gratings and surface waves allows us to actively modulate thermal radiation. The anomalous properties of the devices utilizing resonant gratings are summarized in Section 5.

2. Optical Analysis

We develop a modal analysis⁽¹⁹⁻²¹⁾ to evaluate the optical responses of gratings. The coordinate system for the analysis is shown in **Fig. 1**. For simplicity, we limit the p-polarized incidence in the xz plane. As a result, the following condition is satisfied:

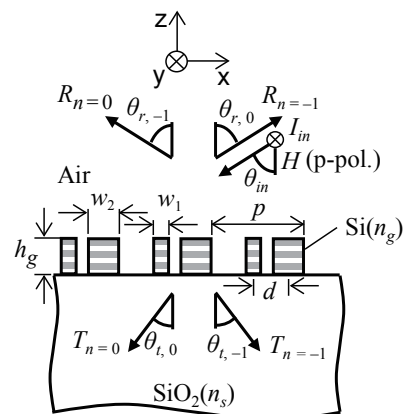


Fig. 1 Configuration of the Littrow mounted double-groove grating. (dimensions: $p = 895$ nm, $w_1 = 200$ nm, $w_2 = 300$ nm, $d = 360$ nm, and $h_g = 1030$ nm; refractive indexes: $n_s = 1.45$ and $n_g = 3.48$; diffraction angles: $\theta_{r,0} = \theta_{r,-1} = 60^\circ$ and $\theta_{t,0} = \theta_{t,-1} = 36.7^\circ$ at $\lambda_0 = 1550$ nm operating wavelength).

$$H_x = H_z = E_y = 0, \quad (1)$$

where H_j is the j -component of the magnetic field and E_j is the j -component of the electric field. Since E_x and E_z are derived from H_y , only H_y is considered in the following discussion. In the grating layer, the magnetic field $H_y^{(G)}$ is decomposed by eigenmodes as follows:

$$H_y^{(G)} = \sum_m X_m(x) [U_m^{(G)} \exp(iA_m z) + D_m^{(G)} \exp(-iA_m z)], \quad (2)$$

where A_m and $X_m(x)$ are the m th eigenvalue and eigenfunction, and $U_m^{(G)}$ and $D_m^{(G)}$ are amplitudes of the m th mode. In the other homogenous layers, the electromagnetic field is decomposed by plane waves, i.e., Rayleigh expansion. In the semifinite input layer, the magnetic field $H_y^{(IN)}$ is written as the sum of the incidence and the reflection:

$$H_y^{(IN)} = H_m \exp(-i\beta_0 x - i\gamma_0^{(IN)} z) + \sum_n H_{Rn} \exp(-i\beta_n x + i\gamma_n^{(IN)} z), \quad (3)$$

where H_m is the incident magnetic field, H_{Rn} is the reflected magnetic field of the n th order diffraction, β_0 is the x -component of the incident wavevector, β_n is the x -component of the n th diffracted order wavevector $\beta_n = \beta_0 + n(2\pi/p)$, p is the period of the grating, and $\gamma_n^{(IN)}$ is the z -component of the wavevector of the n th order diffraction. In the semifinite substrate, the field $H_y^{(SUB)}$ is written as the sum of the transmission in a similar manner:

$$H_y^{(SUB)} = \sum_n H_{Tn} \exp(-i\beta_n x - i\gamma_n^{(SUB)} z), \quad (4)$$

where H_{Tn} is the transmitted magnetic field of the n th order diffraction. Four variables, namely, the optical responses of the structure H_{Rn} and H_{Tn} , and the internal magnetic field $U_m^{(G)}$ and $D_m^{(G)}$, are determined by solving four equations derived from boundary conditions at the two interfaces of the three layers. A similar procedure is applied to structures with more layers. The calculated optical responses are verified by using the commercial electromagnetic simulator CST Microwave Studio™ (22)

3. Asymmetric Double-groove Grating for Light Manipulation

Reflection gratings coupled to nonzero-order diffraction beams are key devices for applications requiring angular

dispersion, e.g., spectrometers, lasers, and filters. They are commonly realized by metallic gratings or dielectric gratings attached onto multilayered dielectric mirrors⁽²³⁻²⁶⁾ or metallic mirrors.⁽²⁷⁾ We have reported a resonant grating coupled to the -1 st-order diffraction with an efficiency as high as unity,⁽⁵⁾ unlike other resonant gratings,⁽¹⁰⁻¹⁸⁾ which focus on the 0th order. It consists of two silicon ridges with different widths placed on a fused quartz substrate. Reflective coupling is achieved without attaching a mirror on the backside as in other studies.⁽²³⁻²⁶⁾ Another unique feature of this device, the alternation of reflection and transmission by changing incident angle from $+60^\circ$ to -60° , is discussed at the end of this section.

The configuration of the silicon double-groove grating on the fused quartz substrate is shown in Fig. 1. The geometry of the grating is optimized so as to achieve unity efficiency for 1550 nm signal light incident at 60° . The angle of the -1 st-order reflection is designed to be the same as the angle of incidence, i.e., Littrow mounting is utilized. Thus, the incoming light is reflected back in the incoming direction.

The wavelength characteristics of the diffraction efficiency calculated by the modal analysis are shown in Fig. 2. As mentioned above, the efficiency for the -1 st-order coupling at 1550 nm is almost unity. The spectral bandwidth is relatively narrow, which implies a resonance in the structure. The simulated results obtained by CST Microwave Studio™ are shown as dots in Fig. 2 and capture the calculated efficiency by the modal analysis.

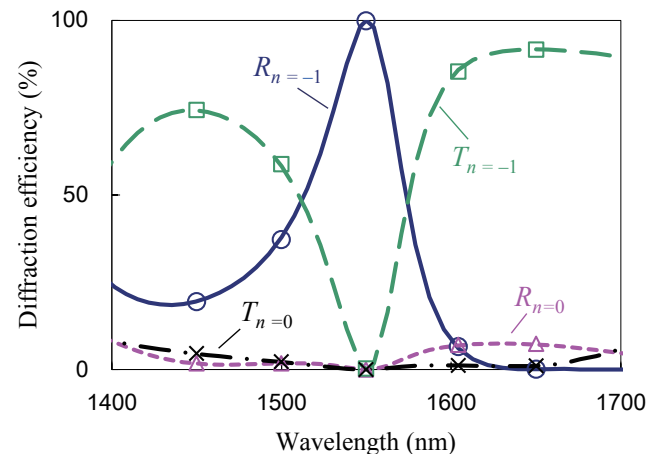


Fig. 2 Wavelength characteristic of diffraction efficiencies in the Littrow mounted double-groove grating. Curves are obtained using the modal analysis. Data points are the results of the CST Microwave Studio™ simulation.

The angular characteristics of the diffraction efficiency at 1550 nm are shown in Fig. 3. A high efficiency of over 70% is obtained for incidence from 50° to 75°. The efficiency is zero at angles below 47° because the -1st-order diffraction does not propagate into the free space, i.e., the -1st-order diffraction is evanescent wave.

The electromagnetic field in the grating is shown in Fig. 4. As mentioned above, the incidence from +60° couples to the -1st-order reflection. Simultaneously, the incidence excites a strong magnetic field inside the wider ridge, as seen in Fig. 4(a). By contrast, the incidence from -60° couples to the -1st-order transmission with high efficiency (Fig. 4(b)). This switching between reflection and transmission cannot be achieved by gratings with backside-attached mirrors.

4. Resonant Grating for Thermal Radiation Control

Thermal radiation has been considered to be a broadband phenomenon since the complete explanation of the blackbody radiation by Plank. From a realistic non-blackbody structure, the spectral radiance of thermal radiation $B_\lambda(\lambda, \theta, T)$, measured in units of $W \cdot sr^{-1} \cdot m^{-3}$, can be expressed as the product of Planck's oscillator and the emissivity $\varepsilon(\lambda, \theta)$ at a specific wavelength λ and angle θ :

$$B_\lambda(\lambda, \theta, T) = \frac{2hc^2}{\lambda^5} \frac{1}{\exp(hc/\lambda k_B T) - 1} \varepsilon(\lambda, \theta), \quad (5)$$

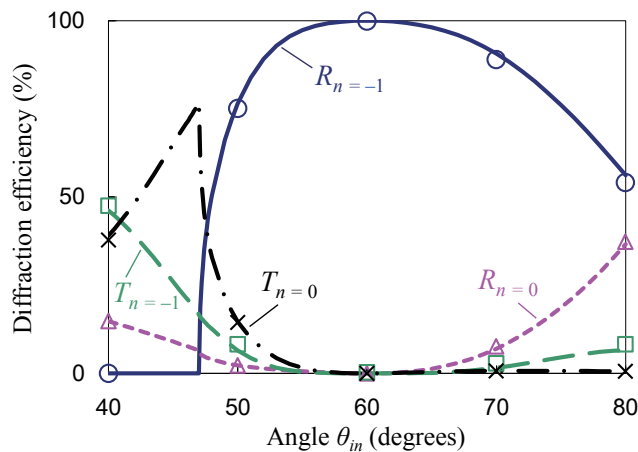


Fig. 3 Incident angle dependence of diffraction efficiencies in the Littrow mounted double-groove grating. Curves are obtained using the modal analysis. Data points are the results of the CST Microwave Studio™ simulation.

where h is Planck's constant, c is the speed of light, k_B is the Boltzmann constant, and T is the temperature. Tailoring emissivity by subwavelength structures for thermal radiation control is currently attracting much interest. Several applications have been proposed, including chemical analysis,⁽²⁸⁾ cooling systems,^(29,30) and thermophotovoltaics.⁽³¹⁾ Various types of structures including photonic crystals,⁽³²⁾ surface relief gratings,^(33,34) and metamaterials^(35,36) have been investigated both theoretically and experimentally. We have reported that resonant gratings coupled to surface phonon polaritons on the SiC substrate achieve spectrally and angularly sharp thermal radiation characteristics.⁽⁶⁾ The characteristics of the proposed structure are analyzed according to Kirchhoff's law.⁽³⁷⁾ The absorptivity $\alpha(\lambda, \theta)$ at a specific wavelength and angle is calculated analytically or numerically. Then, emissivity is derived via the equation $\alpha(\lambda, \theta) = \varepsilon(\lambda, \theta)$.

The configuration of the proposed thermal radiator is shown in Fig. 5 (a). The thermal energy from the SiC substrate excites surface phonon polaritons on the substrate. Surface polaritons couple to the guided modes in the dielectric resonant grating. The guided modes couple to the propagative wave above the grating,

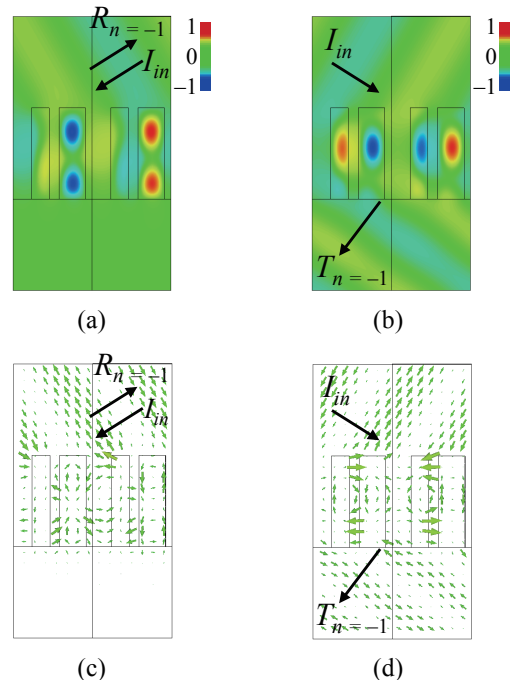


Fig. 4 Snap shot of electromagnetic field distributions at 1550 nm obtained by the CST Microwave Studio™ simulation. (a) +60° incidence (magnetic field) (b) -60° incidence (magnetic field) (c) +60° incidence (electric field) (d) -60° incidence (electric field).

and thus thermal radiation is observed at a specific wavelength and angle where the surface polaritons are excited and the coupling condition is satisfied. Such properties are observed in the spectral and angular emissivity plotted in Fig. 6. A near-unity emissivity is achieved around a wavelength of 12.13 μm and the normal direction. There are also lines with high emissivity related to the guided modes or the surface phonon polaritons.

Next, we discuss the active modulation capability of the proposed structure. The emissivity is modulated by tuning the distance between the substrate and the grating, shown as the red line in Fig. 7. The emissivity is reduced from almost unity to zero by increasing the distance from 36.15 μm to 37.3 μm . To elucidate the dependence on distance, we employed an approximation that disregards the propagative wave between the grating and the substrate. This approximation, which is represented by the blue dashed line in Fig. 7, shows the contribution of the evanescent wave. The approximation captures the envelope of the emissivity, which indicates that the coupling is dominated by the evanescent wave. The dip could be explained as the interference of the propagative and evanescent waves.

Furthermore, we achieved spatially asymmetric thermal radiation by utilizing the asymmetric double-groove reflective grating discussed in Section 3, as shown in Fig. 8(a). We modified the geometrical

parameters so as to satisfy the coupling condition, and achieved almost unity emissivity toward the right hand side (Fig. 8(b)). This is due to the excitation of the surface phonon polariton and the guided mode. Toward the left hand side, the emissivity is almost zero (Fig. 8(c)). This asymmetry is visualized in Fig. 8(d) in terms of the spectral and angular characteristics.

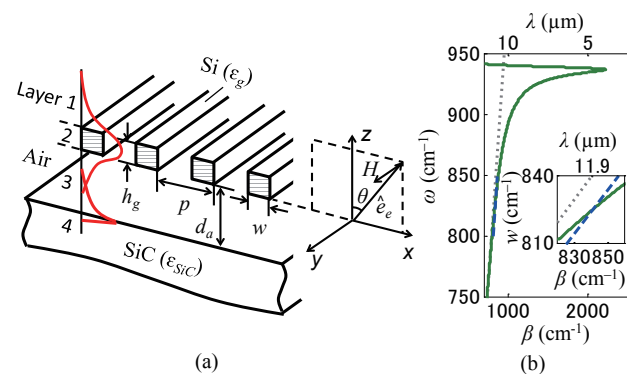


Fig. 5 (a) Sketch of a thermal emitter. It consists of a silicon resonant grating positioned above a silicon carbide (SiC) plate. (dimensions: $p = 11.9 \mu\text{m}$, $w = 5.7 \mu\text{m}$, $h_g = 1.01 \mu\text{m}$, $d_a = 36.2 \mu\text{m}$; permittivities: $\epsilon_g = 12.1$, ϵ_{SiC} is given in Ref. (31)) (b) Dispersion curves of surface phonon polaritons on the surface of a SiC plate (green solid line) and the guided mode of the resonant grating (blue dashed line) and the light line (gray dotted line).

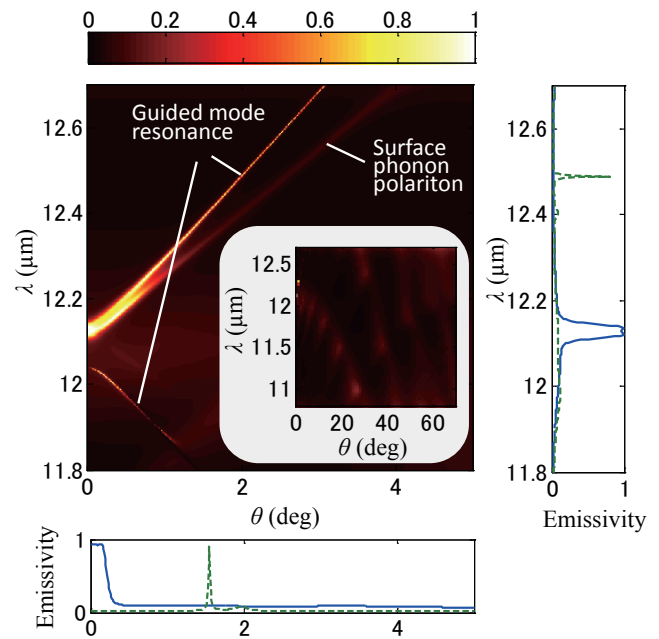


Fig. 6 Spectral emissivity with variation of the angle θ in the xz plane for p-polarization. The graph on the bottom plots emissivity vs. angle θ at 12.13 μm (blue solid line) and 12.4 μm (green dashed line). The graph on the right plots emissivity vs. λ at $\theta = 0^\circ$ (blue solid line) and $\theta = 2^\circ$ (green dashed line).

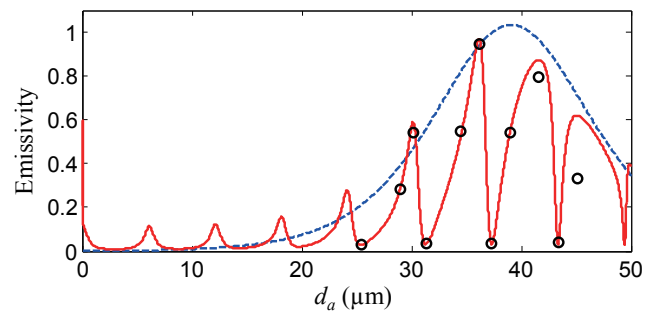


Fig. 7 Emissivity as a function of distance, d_a , at $\lambda = 12.13 \mu\text{m}$ and $\theta = 0^\circ$. (Red solid line: modal analysis; black circles: CST Microwave Studio™; blue dashed line: approximation.)

5. Summary

An asymmetric optical component and a thermal radiator based on resonant gratings were reviewed. The optical responses of the both devices were analyzed by the modal analysis. The reflective or

transmissive coupling to the -1st-order diffraction was observed on the asymmetric double-groove grating. It finds applications such as signal routing based on light switching, laser pulse compression, laser cavities, and so on. The sharp spectral and angular radiation characteristics as well as the modulation capability were investigated on the thermal radiator. Spatially asymmetric thermal radiation was also demonstrated. It is applicable to thermal management, thermophotovoltaics, and mid-infrared optical sources. The methodologies for designing and analyzing dielectric resonant gratings contribute to the fields of optics and thermal radiation.

References

- (1) Iizuka, H. et al., "Incident Angle Dependency of Propagating Modes in Rectangular Grating for Polarization-independent -1st Order Diffraction or Polarization Splitting", *Micro. Opt. Tech. Lett.*, Vol. 52, No. 6 (2010), pp. 1362-1369.
- (2) Iizuka, H. et al., "Switching Capability of Double-sided Grating with Horizontal Shift", *Appl. Phys. Lett.*, Vol. 97, No. 5 (2010), 053108.
- (3) Iizuka, H. et al., "Role of Propagating Modes in a Double-groove Grating with a +1st-order Diffraction Angle Larger than the Substrate-air Critical Angle", *Opt. Lett.*, Vol. 35, No. 23 (2010), pp. 3973-3975.
- (4) Inoue, D. et al., "Polarization Filters for Visible Light Consisting of Subwavelength Slits in an Aluminum Film", *J. Lightwave Tech.*, Vol. 30, No. 22 (2012), pp. 3463-3467.
- (5) Ito, K. and Iizuka, H., "Highly Efficient -1st-order Reflection in Littrow Mounted Dielectric Double-groove Grating", *AIP Adv.*, Vol. 3, No. 6 (2013), 062119.
- (6) Ito, K. et al., "Thermal Emission Control by Evanescent Wave Coupling between Guided Mode of Resonant Grating and Surface Phonon Polariton on Silicon Carbide Plate", *Appl. Phys. Lett.*, Vol. 104, No. 5 (2014), 051127.
- (7) Matsui, T. et al., "Experimental Investigation of Double-groove Grating Satisfying Total Internal Reflection Condition", *Opt. Express*, Vol. 22, No. 21 (2014), pp. 25362-25370.
- (8) Iizuka, H. et al., "Light Manipulation with Dielectric Gratings", *R&D Review of Toyota CRDL*, Vol. 43, No. 3 (2012), pp. 69-75.
- (9) Inoue, D. et al., "Optical Filters Using Metal-based Metamaterial", *R&D Review of Toyota CRDL*, Vol. 45, No. 1 (2014), pp. 9-16.
- (10) Magnusson, R. and Wang, S. S., "New Principle for Optical Filters", *Appl. Phys. Lett.*, Vol. 61, No. 9 (1992), pp. 1022-1024.
- (11) Wang, S. S. and Magnusson, R., "Theory and Applications of Guided-mode Resonance Filters",

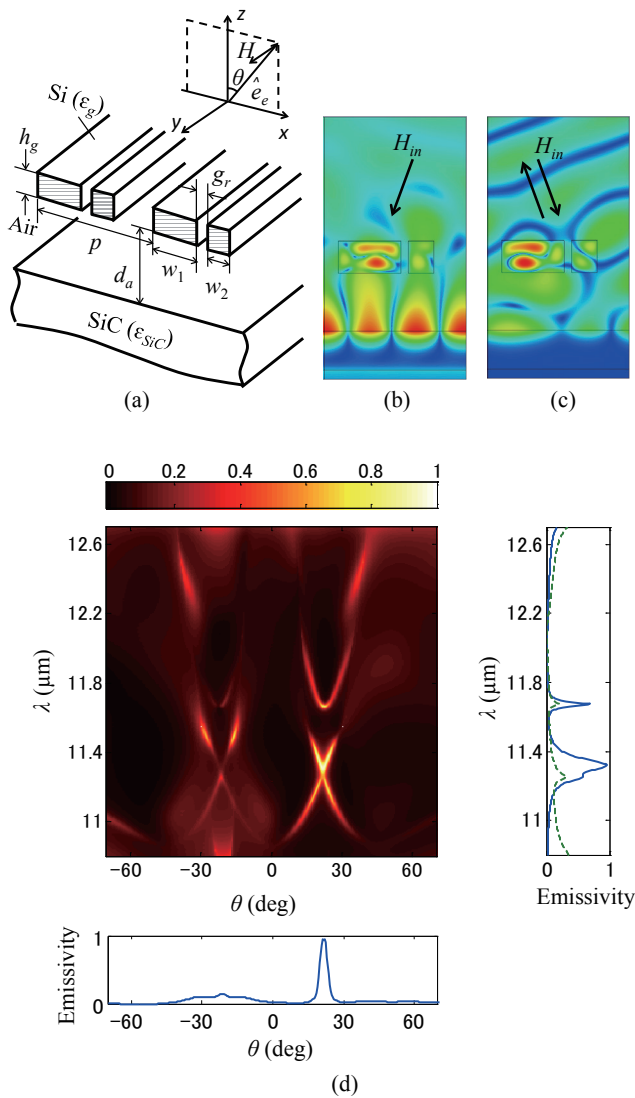


Fig. 8 (a) Sketch of the thermal emitter having a silicon double-groove grating with two different groove widths per period. (Dimensions: $p = 15.4 \mu\text{m}$, $w_1 = 6.8 \mu\text{m}$, $w_2 = 2.8 \mu\text{m}$, $h_g = 3.5 \mu\text{m}$, $g_r = 0.8 \mu\text{m}$, and $d_a = 6.3 \mu\text{m}$.) Magnetic field intensity $|H_y|$ distributions for (b) $\theta = +21^\circ$ and (c) $\theta = -21^\circ$, obtained using the CST Microwave Studio™ simulation. (d) Spectral emissivity with variation of the angle θ in the xz plane for p-polarization. Emissivity vs. angle θ at $11.32 \mu\text{m}$ and emissivity vs. λ for $\theta = +21^\circ$ (blue solid line) and $\theta = -21^\circ$ (green dashed line) are plotted in the bottom and the right graphs, respectively.

- Appl. Opt.*, Vol. 32, No. 14 (1993), pp. 2606-2613.
- (12) Brundrett, D. L. et al., "Normal-incidence Guided-mode Resonant Grating Filters: Design and Experimental Demonstration", *Opt. Lett.*, Vol. 23, No. 9 (1998), pp. 700-702.
- (13) Brundrett, D. L. et al., "Effects of Modulation Strength in Guided-mode Resonant Subwavelength Gratings at Normal Incidence", *J. Opt. Soc. Am. A*, Vol. 17, No. 17 (2000), pp. 1221-1230.
- (14) Kanamori, Y. et al., "Control of Guided Resonance in a Photonic Crystal Slab Using Microelectromechanical Actuators", *Appl. Phys. Lett.*, Vol. 90, No. 3 (2007), 031911.
- (15) Foley, J. M. et al., "Narrowband Mid-infrared Transmission Filtering of a Single Layer Dielectric Grating", *Appl. Phys. Lett.*, Vol. 103, No. 7 (2013), 071107.
- (16) Huang, M. C. Y. et al., "A Surface-emitting Laser Incorporating a High-index-contrast Subwavelength Grating", *Nature Photonics*, Vol. 1 (2007), pp. 119-122.
- (17) Huang, M. C. Y. et al., "A Nanoelectromechanical Tunable Laser", *Nature Photonics*, Vol. 2 (2008), pp. 180-184.
- (18) Fattal, D. et al., "Flat Dielectric Grating Reflectors with Focusing Abilities", *Nature Photonics*, Vol. 4 (2010), pp. 466-470.
- (19) Sheng, P. et al., "Exact Eigenfunctions for Square-wave Gratings: Application to Diffraction and Surface-plasmon Calculations", *Phys. Rev. B*, Vol. 26 (1982), pp. 2907-2917.
- (20) Li, L., "A Modal Analysis of Lamellar Diffraction Gratings in Conical Mountings", *J. Mod. Opt.*, Vol. 40, No. 4 (1993), pp. 553-573.
- (21) Clausnitzer, T. et al., "An Intelligible Explanation of Highly-efficient Diffraction in Deep Dielectric Rectangular Transmission Gratings", *Opt. Express*, Vol. 13, No. 26 (2005), pp. 10448-10456.
- (22) CST Microwave Studio 2013, <<http://www.cst.com>> (accessed 2013-12-01).
- (23) Perry, M. D. et al., "High-efficiency Multilayer Dielectric Diffraction Gratings", *Opt. Lett.*, Vol. 20, No. 8 (1995), pp. 940-942.
- (24) Hehl, K. et al., "High-efficiency Dielectric Reflection Gratings: Design, Fabrication, and Analysis", *Appl. Opt.*, Vol. 38, No. 30 (1999), pp. 6257-6271.
- (25) Wei, H. and Li, L., "All-dielectric Reflection Gratings: A Study of the Physical Mechanism for Achieving High Efficiency", *Appl. Opt.*, Vol. 42, No. 31 (2003), pp. 6255-6260.
- (26) Destouches, N. et al., "99% Efficiency Measured in the -1st Order of a Resonant Grating", *Opt. Express*, Vol. 13, No. 9 (2005), pp. 3230-3235.
- (27) Hu, A. et al., "Modal Analysis of High-efficiency Wideband Reflective Gratings", *J. Opt.*, Vol. 14, No. 5 (2012), 055705.
- (28) Miyazaki, H. et al., "Thermal Emission of Two-color Polarized Infrared Waves from Integrated Plasmon Cavities", *Appl. Phys. Lett.*, Vol. 92, No. 14 (2008), 141114.
- (29) Rephaeli, E. et al., "Ultrabroadband Photonic Structures to Achieve High-performance Daytime Radiative Cooling", *Nano Lett.*, Vol. 13, No. 4 (2013), pp. 1457-1461.
- (30) Raman, A. et al., "Passive Radiative Cooling Below Ambient Air Temperature under Direct Sunlight", *Nature*, Vol. 515, No. 7528 (2014), pp. 540-544.
- (31) Sai, H. et al., "High-temperature Resistive Surface Grating for Spectral Control of Thermal Radiation", *Appl. Phys. Lett.*, Vol. 82, No. 11 (2003), pp. 1685-1687.
- (32) Inoue, T. et al., "Realization of Dynamic Thermal Emission Control", *Nature Materials*, Vol. 13 (2014), pp. 928-931.
- (33) Greffet, J. J. et al., "Coherent Emission of Light by Thermal Sources", *Nature*, Vol. 416 (2002), pp. 61-64.
- (34) Arnold, C. et al., "Coherent Thermal Infrared Emission by Two-dimensional Silicon Carbide Gratings", *Phys. Rev. B*, Vol. 86 (2012), 035316.
- (35) Liu, X. et al., "Taming the Blackbody with Infrared Metamaterials as Selective Thermal Emitters", *Phys. Rev. Lett.*, Vol. 107 (2011), 045901.
- (36) Mason, J. A. et al., "Strong Absorption and Selective Thermal Emission from a Midinfrared Metamaterial", *Appl. Phys. Lett.*, Vol. 98, No. 24 (2011), 241105.
- (37) Greffet, J. J. and Nieto-Vesperinas, M., "Field Theory for Generalized Bidirectional Reflectivity: Derivation of Helmholtz's Reciprocity Principle and Kirchhoff's Law", *J. Opt. Soc. Am. A*, Vol. 15, No. 10 (1998), pp. 2735-2744.
- Figs. 1-4
Reprinted from AIP Advances, Vol. 3 (2013), 062119, Ito, K. et al., Highly-efficient -1st-order Reflection in Littrow Mounted Dielectric Double-groove Grating, © 2013 AIP.
- Figs. 5-8
Reprinted from Applied Physics Letters, Vol. 104 (2014), 051127, Ito, K. et al., Thermal Emission Control by Evanescent Wave Coupling between Guided Mode of Resonant Grating and Surface Phonon Polariton on Silicon Carbide Plate, © 2014 AIP, with permission from AIP Publishing LLC.

Kota Ito

Research Fields:

- Nanophotonics
- Nanoscale Heat Transfer

Academic Societies:

- The Japan Society of Applied Physics
- The Institute of Electrical Engineers of Japan



Takayuki Matsui

Research Fields:

- Optics
- Nanophotonics

Academic Societies:

- The Japan Society of Applied Physics
- The Optical Society of America



Hideo Iizuka

Research Field:

- Electromagnetic Analysis

Academic Degree: Dr.Eng.

Academic Societies:

- IEEE
- The Optical Society of America
- The Institute of Electronics, Information and Communication Engineers

Award:

- IEICE Young Engineer. Award, 2001

